Effect of Nd^{3+} Concentration on the Physical and Absorption Properties of Sodium-Lead-Borate Glasses

S. Mohan^{*,a}, K. S. Thind^{b}, and G. Sharma^{b}
^{a}Lecturer in Physics, BBK DAV College for Women, Amritsar, India
^{b}Department of Physics, Guru Nanak Dev University, Amritsar, India

The effect of increasing the rare earth ion concentration on the physical and spectroscopic properties of Nd^{3+} doped sodium-lead-borate glasses have been studied for the compositions (10-x) Na$_2$O–30PbO–60B$_2$O$_3$–xNd$_2$O$_3$, where x = 1.00, 1.25, 1.50, 1.75 and 2.00 mol %. Optical band gaps, cut-off wavelengths and various spectroscopic parameters (E^1, E^2, E^3, F$_2$, F$_4$, F$_6$ and ξ_{4f}) have been determined from the room temperature absorption spectra. Judd-Ofelt theory has been employed to determine the intensity parameters Ω_2, Ω_4 and $\Omega_6$which in turn are used to evaluate radiative transition probability (A), branching ratio (β) and radiative lifetime (τ_R) for the fluorescent level ^{4}F$_{3/2}$. The Ω_2 parameter and hence the non-symmetric component of electric field acting on Nd^{3+} ion is found to be highest for glass with 1.75 mol% of Nd$_2$O$_3$. Because of the poor resolution of hypersensitive transition, the covalency of the Nd-O bond has been characterized by the relative intensity of ^{4}I$_{9/2}$ →^{4}F$_{7/2}$, ^{4}S$_{3/2}$. The highest covalency has been predicted for glass with 2 mol% Nd$_2$O$_3$. The radiative properties are found to improve with an increase in concentration of Nd$_2$O$_3$ for the present study.

Keywords: Optical materials; Glasses; Optical properties; Judd-Ofelt theory

I. INTRODUCTION

Physical and spectroscopic properties of silicate, borate and phosphate glasses doped with various rare earth (RE^{3+}) ions have been extensively investigated in the past, and many technological and commercial applications have been realized [1-4]. Neodymium has been most widely studied as doping agent and has come out to be most applicable for laser action, since neodymium lasers can operate with high efficiency, even at room temperature.

Since, a maximum laser output requires an optimum concentration of Nd^{3+} it becomes important to study the spectroscopic properties as a function of concentration of rare earth ions. Both higher and lower concentrations lead to lower laser efficiencies. The lower efficiencies at higher concentrations are due to nonradiative self-quenching process.

Borate glass is a particularly suitable optical material because of its high transparency, low melting point, high thermal stability, different coordination numbers, and good solubility of rare-earth ions [5–6]. Further, heavy metal oxide glasses have reduced phonon energy. Thus, the incorporation of heavy metal oxides such as PbO or Bi$_2$O$_3$ into the borate glass matrix leads to an increase in its quantum efficiency of luminescence from the excited states of rare-earth ions. Further, RE-doped alkali borate glasses are interesting for studying effects of alkali ions on the glass forming network, particularly around the rare-earth ions. It is well established that the addition of an alkali oxide has a strong influence on the boron coordination and the structural groups, depending on the type and concentration of the alkali oxide [7].

Saisudha et al. [8] have investigated the effect of the lead borate matrix on the optical properties of the Nd^{3+} ions. Large stimulated emission cross sections have been reported [9] stressing the suitability of different Nd^{3+} doped lead borate and bismuth borate glasses for laser action. Studies of NMR and fluorescence of Nd^{3+} doped binary alkali borate glasses have also been published [10, 11]. However, to the best of our knowledge, rare earth doped alkali lead borate glasses have not been studied in any great detail. Motivated by these considerations we have prepared sodium-lead borate glasses doped with Nd^{3+}, and studied the effects of the Nd^{3+} concentration on physical and spectroscopic properties.

II. EXPERIMENTAL

A series of Nd^{3+} doped sodium-lead-borate glasses of the type (10-x) Na$_2$O–30PbO–60B$_2$O$_3$–xNd$_2$O$_3$, where x = 0.5, 1.0, 1.5 and 2 mol % were prepared by the melt quenching technique. Appropriate amounts of the raw materials, Na$_2$CO$_3$, PbO, B$_2$O$_3$ and Nd$_2$O$_3$ of 99.9 % purity, were thoroughly mixed and ground in an agate mortar in 20 g batches. The prepared batches were heated in a silica crucible at 450–500 ^{o}C for 2 hours to ensure decarbonisation of the sodium carbonate. The temperature was then raised and maintained at 1000 ^{o}C for about one hour. The mixture was occasionally stirred to ensure homogeneous mixing of all constituents and to obtain bubble-free samples. Finally, the mixture was poured into a preheated brass mould and annealed near the glass transition temperature in order to eliminate internal mechanical stress. Samples of good optical quality were selected and sliced, grinded and polished in order to study their spectroscopic properties. The chemical compositions of the samples are summarized in Table 1.

By applying Archimedes principle, the densities of the prepared samples were measured with benzene as the immersion liquid. The density was calculated using the formula:

$$\rho = \frac{W_a}{W_a - W_b} \times \rho_b \qquad (1)$$

where $W_a$is the weight in air, W_b is the weight in benzene, and

TABLE I: Chemical composition of glasses

Glass	Composition in mol %			
	Na$_2$O	PbO	B$_2$O$_3$	Nd$_2$O$_3$
NPBN1	9.00	30	60	1.00
NPBN2	8.75	30	60	1.25
NPBN3	8.50	30	60	1.50
NPBN4	8.25	30	60	1.75
NPBN5	8.00	30	60	2.00

TABLE II: Physical properties of sodium-lead-borate glasses containing varying amounts of Nd^{3+} ions.

Physical property	Glass Sample				
	NPBN1	NPBN2	NPBN3	NPBN4	NPBN5
Refractive index (n)	1.652	1.652	1.652	1.652	1.652
Density (ρ) (g/cm^3)	4.24	4.36	4.55	4.48	4.51
Average molecular weight ($\bar{M}$) (g)	117.59	118.26	118.93	119.59	120.26
Molar Volume (V_M) (cm^3)	27.69	27.11	26.14	26.68	26.67
Ion concentration N ($\times 10^{20}$ ions/cm^3)	4.35	5.55	6.91	7.90	9.03
Ion concentration c(moles/liter)	0.72	0.92	1.15	1.31	1.50
Polaron radius r_p (Å)	5.32	4.90	4.56	4.36	4.17
Field Strength F ($\times 10^{15}$cm^2)	1.06	1.25	1.44	1.58	1.73
Inter nuclear distance r_i (Å)	13.20	12.16	11.31	10.81	10.34
Dielectric constant (ε)	2.73	2.73	2.73	2.73	2.73
Molar refraction (R_M)	10.12	9.91	9.56	9.76	9.75
Reflection losses (R %)	6.04	6.04	6.04	6.04	6.04

ρ_b is the density of benzene. All weight measurements were made using a Dhona single pan balance.

The refractive index was measured at a temperature of 30 ^{o}C, with an Abbe refractometer using mono-bromonaphthalene as adhesive coating. Optical absorption spectra were recorded at room temperature using a spectrophotometer (Shimadzu), working in the UV-visible range.

III.   RESULTS AND DISCUSSION

A.   Physical properties

The physical properties provide an insight into the atomic arrangements in a glass network. The concentration of the rare-earth ions is an important parameter, which affects the laser gain of the host material. The number density N of the laser-active ions i.e. the number of ions per cubic centimeter can be evaluated using the relation [12]

$$N(ions/cm^3) = \frac{x\rho N_A}{\bar{M}} \quad (2)$$

where ρ is the density of the glass, N_A is the Avagadro's number, x is the mole fraction of rare earth oxide and $\bar{M}$ is the average molecular weight of the glass.

Some other physical properties which include molar volume (V_M), polaron radius (r_p), internuclear distance (r_i), field Strength (F), dielectric constant (ε) and molar refraction (R_M) were determined from the density, average molecular weight, refractive index and concentration of the rare-earth ions, using standard formulae [12]. All the above mentioned physical properties are listed in Table 2.

The density is found to increase with the increase in concentration of Nd^{3+} ions upto 1.5 mol% of Nd$_2$O$_3$. It then decreases for 1.75 mol% and then again shows an increase for higher concentration of Nd$_2$O$_3$. A possible reason of decrease in density could be the formation of non-bridging oxygen (NBO's) atoms around 1.75 mol% concentration of neodymium oxide. The clustering of rare earth ions can be one of the factors which contribute to the variation in density at higher concentrations. The behavior of molar volume mainly depends upon the density of glasses and as expected in the present case, it follows a trend opposite to density. The variation of density and molar volume with concentration of Nd$_2$O$_3$ is presented in Fig. 1.
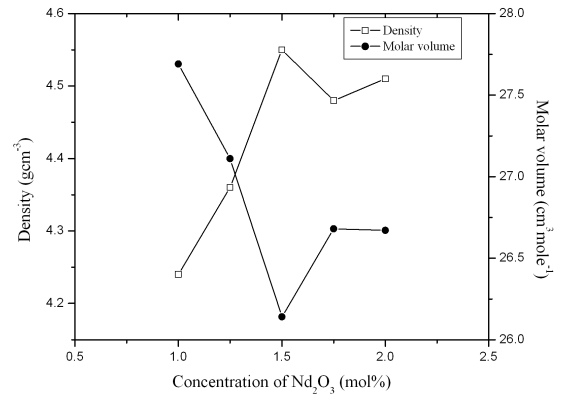
FIG. 1: Variation of density and molar volume with the concentration of Nd$_2$O$_3$.

The polaron radius is found to decrease with the increase in neodymium oxide content. This result agrees with the literature [13]. The internuclear distance for rare earth ions shows an expected decrease on increasing Nd$_2$O$_3$ content. The molar refraction, which depends on the refractive index, density and average molecular weight of glass, shows a minimum around 1.5 mol% of Nd$_2$O$_3$.

B.   Energy band gap and cut-off wavelength

Optical absorption spectrum of Nd^{3+} doped sodium-lead-borate glass in the wavelength range 400–950 nm is shown in Fig. 2. This sample contains 1 mol% Nd_2O_3. Spectra of other samples are similar in shape with small differences in absorbance.
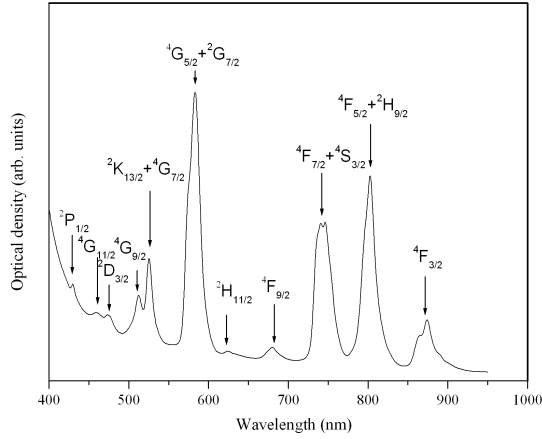
FIG. 2: Room temperature absorption spectra of sodium-lead-borate glass containing 1mol% of Nd_2O_3.

Optical band gaps for direct and indirect transitions have been obtained following Mott and Davis [14], using the equation

$$\hbar\omega\alpha(\omega) = B\left[\hbar\omega - E_0\right]^n \qquad (3)$$

where B is a constant, α is the absorption coefficient, ω is the angular frequency and values of n are $1/2$ and 2 for direct and indirect transitions respectively.

To calculate the width of the energy tail, ΔE, of the density of states, the model proposed by Urbach [15] and Tauc [16] is followed. The following relation has been used to determine the width of the energy tail:

$$\ln\left(\alpha\right) = C + \frac{\hbar\omega}{\Delta E} \qquad (4)$$

where C is a constant.

Values of direct and indirect mobility gap, width of mobility tail and the cut-off wavelength for the present glass system are presented in Table 3. The indirect and direct mobility gap both show a maximum for 2 mol% and a minimum for 1mol% concentration of Nd_2O_3. The direct mobility gap shows an increase upto 1.5 mol%, decreases for 1.75 mol% and then again shows an increase. The indirect mobility gap does not follow a uniform variation. The variations of cut-off wavelength agree with the trend followed by direct mobility gap. The cut-off wavelength for various concentrations of Nd^{3+} in sodium-lead-borate glasses is presented in Fig. 3.

TABLE III: Optical band gaps, width of tail and cut-off wavelength for glasses.

Parameter	Glass Sample				
	NPBN1	NPBN2	NPBN3	NPBN4	NPBN5
Indirect mobility gap E_{ind} (eV)	3.14	3.23	3.21	3.24	3.37
Direct mobility gap E_{dir} (eV)	3.32	3.40	3.44	3.42	3.50
Width of tail (ΔE) (eV)	0.19	0.15	0.15	0.08	0.06
Cut-off Wavelength (nm)	373	368	362	363	361
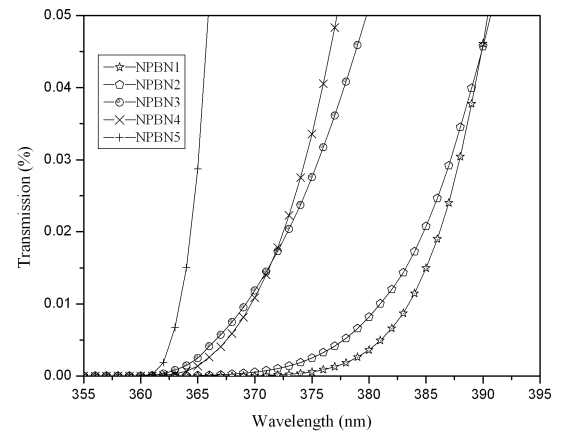
FIG. 3: Cut-off wavelength for sodium-lead-borate glasses containing varying amounts of Nd_2O_3.

C.   Absorption spectroscopic parameters

A comparison of the optical absorption spectra of the present glass series with the standard wavelength chart of Nd^{3+} [17], result in the identification of following spectroscopic transitions:

$^4F_{3/2}$, $^4F_{5/2} +^2 H_{9/2}$, $^4S_{3/2} +^4 F_{7/2}$, $^4F_{9/2}$, $^2H_{11/2}$, $^4G_{5/2} +^2 G_{7/2}$, $^2K_{13/2} +^4 G_{7/2}$, $^4G_{9/2}, ^2D_{3/2}$, $^4G_{11/2}$, $^2P_{1/2}$ $\leftarrow$ $^4I_{9/2}$.

Using the observed band energies as E_J and the zero point energies (E_{0J}) and partial derivates [18], the correction factors ΔE^k and $\Delta \xi_{4f}$ have been evaluated by the least –squares fit method. The calculated correction factors are then added to the zero-order parameters [18] to obtain the Racah parameters (E^k) and the spin-orbit interaction parameter (ξ_{4f}). The Slater integrals (F^k) have been evaluated from Racah parameters using relevant expressions [12]. The rms deviations between the energies (E_{th}) calculated using these parameters and the experimental energies (E_{exp}) are within experimental

limits. These energy values are presented in Table 4. The spectroscopic parameters along with hydrogenic ratios E^1/E^3 and E^2/E^3 determined for different concentrations of Nd^{3+} are presented in Table 5. The, hydrogenic ratios which indicate the radial properties of Nd^{3+}, are approximately the same for all compositions, indicating that the radial properties of Nd^{3+} remain unperturbed with the change in rare earth ion concentration.

D. Spectral intensities and Judd-Ofelt parameters

The intensity of an absorption band can be expressed in terms of the 'oscillator strength'. The experimental oscillator strength (f_{meas}) of the absorption transitions has been determined using [19]

$$f_{\text{meas}} = 4.32 \times 10^{-9} \int \varepsilon(\nu)d\nu, \qquad (5)$$

where $\varepsilon(\nu) = OD/ct$ is the molar extinction coefficient at mean energy ν (cm^{-1}), with OD being the optical density, c being the molar concentration of the rare-earth ions, and t is the optical length of the glass. The intensities for all absorption bands observed in the present case have been evaluated using the area method.

According to Judd-Ofelt theory [20, 21] the oscillator strength of a transition between the initial ground state J manifold $|(S;L)J\rangle$ and a final $J\prime$ manifold $|(S';L')J'\rangle$ can be calculated by the relation:

$$f_{\text{cal}}(aJ,bJ') = \frac{8\pi^2 mc\nu}{3h(2J+1)} \left[\frac{(n^2+2)^2}{9n} S_{\text{ed}} + nS_{\text{md}} \right], \quad (6)$$

where $(2J+1)$ is the degeneracy of the ground state of the Nd^{3+} ions, n is the refractive index of the medium, m is the mass of the electron, and ν is the mean energy of the transition, S_{ed} is the electric dipole line strength and S_{md} is the magnetic dipole line strength. The latter can be neglected in comparison to S_{ed}, since in the present case for Nd^{3+} ion, the bands produced by the magnetic dipole mechanism have very low spectral intensity compared to that of the electric dipole bands. S_{ed} is given by

$$S_{\text{ed}}\left[(S,L)J:(S',L')J'\right] = \sum_{\lambda=2,4,6} \Omega_\lambda \left|\left\langle (S,L)J \left\| U^{(\lambda)} \right\| (S',L')J' \right\rangle\right|^2$$

(7)

where

$$\left|\left\langle (S,L)J \left\| U^{(\lambda)} \right\| (S',L')J' \right\rangle\right|^2 \qquad (8)$$

represents the reduced matrix elements of a unit tensor operator evaluated in the intermediate coupling approximation. Since these reduced matrix elements are host invariant, we have used the values reported by Carnall et al. [22]. The values of experimental and theoretical oscillator strengths along

with their rms deviations are presented in Table 6. The smaller rms deviations indicate good agreement between the experimental and calculated oscillator strengths which shows the validity of Judd-Ofelt theory.

Substituting the oscillator strengths calculated from the absorption spectra for f_{cal}, and using the values of reduced matrix elements and other parameters, the Judd-Ofelt intensity parameters $\Omega_\lambda(\lambda=2,4,6)$ have been determined by least squares method. These parameters along with the intensity parameters of some related borate glasses [29, 8] are presented in Table 7. The table also includes the spectroscopic quality factor (Ω_4/Ω_6), which determines the lasing efficiency of the host.

The position, intensity and shape of certain electric dipole transitions of rare earth ions are found to be very sensitive to the environment of the rare earth ion. Such transitions are termed as hypersensitive transitions by Jorgensen and Judd [23]. These transitions are found to obey the selection rule $\Delta J \leq 2$, $\Delta L \leq 2$ and $\Delta S = 0$ [23]. These transitions are associated with a very large value of the reduced matrix element $\|U^2\|^2$; hence hypersensitivity is much related with the Ω_2 parameter.

For Nd^{3+} ion, $^4I_{9/2} \rightarrow \ ^4G_{5/2} + ^2G_{7/2}$ is the hypersensitive transition since it obeys the required selection rule. As observed from Table, the intensity of hypersensitive transition shows a maximum for 1.75 mol% and a minimum for glass containing 1 mol % of Nd_2O_3. This indicates that the non-symmetric component of electric field acting on Nd^{3+} ion is low for glass containing 1 mol% and high for 1.75 mol% of Nd_2O_3. The possible reason could be the formation of NBO's around 1.75 mol% concentration of Nd_2O_3 as discussed in explaining the density of the present glass system. The creation of non-bridging oxygen from bridging oxygen increases the asymmetry of the bond to the neighboring network cation. A decrease in intensity of hypersensitive transition for 2 mol% Nd_2O_3 glass can be because of clustering of rare earth ions for higher concentrations. The values of Ω_2 are found to be proportional to the intensities of the hypersensitive transition, in accordance with the theory [24].

Krupke [25] pointed out that the transition intensities of $^4I_{9/2} \rightarrow \ ^4G_{5/2} + ^2G_{7/2}$ and $^4I_{9/2} \rightarrow ^4 F_{7/2}$, $^4S_{3/2}$ are determined mainly by Ω_2 and Ω_6 respectively. The Stark splitting due to the crystal field splits these transitions in the absorption spectra into two peaks. The peak intensity ratio of the longer (I_L) and shorter (I_S) wavelength components are designated as I_L/I_S.

In the present case the Stark splitting of the hypersensitive transition $^4I_{9/2} \rightarrow \ ^4G_{5/2} + ^2G_{7/2}$ is poorly resolved. Thus, the Ω_2 parameter is dominated by the crystal-field parameters rather than the covalency parameters. Consequently, no conclusion can be drawn for the covalency of the Nd–O bond using this parameter.

Hence a variation of the spectral profile of the transition $^4I_{9/2} \rightarrow ^4F_{7/2}$, $^4S_{3/2}$ is investigated. This variation is presented in Fig. 4. A higher value of intensity ratio I_L/I_S and intensity parameter Ω_6 indicates a higher covalency of the Nd-O bond for glass containing 2 mol% of Nd_2O_3. A lowest covalency is observed in glass with 1 mol% Nd_2O_3.

TABLE IV: Theoretically calculated and experimentally observed energy levels (cm^{-1}) for various concentrations of Nd^{3+} ions in sodium lead borate glasses.

Levels	NPBN1		NPBN2		NPBN3		NPBN4		NPBN5	
	E_{exp}	E_{th}	E_{exp}	E_{th}	E_{exp}	E_{th}	E_{exp}	E_{th}	E_{exp}	E_{th}
$^4F_{3/2}$	11429	11381	11429	11394	11416	11388	11429	11395	11416	11391
$^4F_{5/2}+^2H_{9/2}$	12439	12470	12438	12460	12438	12456	12438	12467	12438	12464
$^4S_{3/2}+^4F_{7/2}$	13495	13482	13477	13458	13477	13456	13477	13468	13477	13467
$^4F_{9/2}$	14706	14824	14684	14775	14684	14773	14684	14785	14684	14786
$^2H_{11/2}$	16026	16011	15949	15955	15949	15956	15949	15955	15949	15959
$^4G_{5/2}+^2G_{7/2}$	17123	17177	17123	17183	17123	17188	17123	17187	17123	17189
$^2K_{13/2}+^4G_{7/2}$	19011	18935	19011	18925	19011	18918	19011	18913	19011	18912
$^4G_{9/2}$	19493	19540	19493	19508	19493	19508	19493	19521	19493	19520
$^2D_{3/2}+^2G_{9/2}$	21142	21268	21142	21253	21097	21227	21097	21227	21097	21225
$^4G_{11/2}$	21739	21637	21645	21584	21645	21582	21692	21602	21692	21601
$^2P_{1/2}$	23256	23168	23256	23138	23202	23113	23202	23115	23202	23115
rms deviation	±95		±95		±92		±96		±86	

TABLE V: Spectroscopic parameters of Nd^{3+} in sodium-lead-borate glasses.

Parameter	Glass Sample				
	NPBN1	NPBN2	NPBN3	NPBN4	NPBN5
E^1 (cm^{-1})	5018	5020	5009	5008	5011
E^2 (cm^{-1})	25.13	25.02	24.92	24.91	24.88
E^3 (cm^{-1})	485.95	487.41	487.38	487.13	487.16
F^2 (cm^{-1})	332.31	332.41	331.74	331.66	331.63
F^4 (cm^{-1})	47.98	48.26	48.29	48.28	48.39
F^6 (cm^{-1})	5.40	5.37	5.34	5.35	5.35
ξ_{4f} (cm^{-1})	916.13	900.69	903.66	904.77	901.40
E^1/E^3	10.32	10.30	10.27	10.28	10.29
E^2/E^3	0.05	0.05	0.05	0.05	0.05

TABLE VI: Experimental and calculated oscillator strengths of Nd^{3+} doped sodium lead borate glasses.

Transitions from ground state $^4I_{9/2} \rightarrow$	NPBN1		NPBN2		NPBN3		NPBN4		NPBN5	
	f_{exp}	f_{cal}	f_{exp}	f_{cal}	f_{exp}	f_{cal}	f_{exp}	f_{cal}	f_{exp}	f_{cal}
$^4F_{3/2}$	1.32	1.40	1.72	1.76	2.16	1.93	2.24	2.35	2.30	2.44
$^4F_{5/2}+^2H_{9/2}$	4.71	4.44	6.34	6.19	6.74	6.86	7.98	7.64	8.16	8.01
$^4S_{3/2}+^4F_{7/2}$	4.38	4.57	6.59	6.68	7.53	7.43	7.75	7.98	8.23	8.36
$^4F_{9/2}$	0.51	0.38	0.48	0.54	0.70	0.60	0.68	0.66	0.58	0.61
$^2H_{11/2}$	-	-	0.14	0.14	0.14	0.15	0.25	0.17	0.20	0.18
$^4G_{5/2}+^2G_{7/2}$	11.69	11.67	15.25	15.26	17.21	17.19	19.30	19.28	18.31	18.32
$^2K_{13/2}+^4G_{7/2}$	2.36	2.91	3.29	3.82	3.51	4.24	4.10	4.89	4.03	4.31
$^4G_{9/2}$	1.40	0.86	2.02	1.13	2.3	1.25	2.36	1.45	2.49	1.62
$^2D_{3/2}+^2G_{9/2}$	0.48	0.63	0.70	0.84	0.70	0.93	0.89	1.08	0.91	1.11
$^4G_{11/2}$	0.23	0.14	0.49	0.19	0.52	0.21	0.51	0.24	0.61	0.24
$^2P_{1/2}$	0.24	0.35	0.34	0.42	0.41	0.46	0.55	0.58	0.49	0.63
rms deviation	±0.37		±0.39		±0.48		±0.46		±0.37	

TABLE VII: Judd-Ofelt intensity parameters of sodium lead borate glasses doped with various concentrations of Nd^{3+} ions.

Glass matrix	Parameter					Reference
	Ω_2	Ω_4	Ω_6	Ω_4/Ω_6	I_L/I_S	
NPBN1	2.58	2.59	2.98	0.87	1.013	Present work
NPBN2	3.54	3.09	4.41	0.70	1.019	Present work
NPBN3	4.05	3.38	4.71	0.72	1.024	Present work
NPBN4	4.28	4.29	5.23	0.82	1.026	Present work
NPBN5	3.67	4.39	5.50	0.80	1.029	Present work
$30Na_2O+70B_2O_3$	4.91	3.28	4.51	0.72	-	[29]
$30PbO+70B_2O_3$	3.96	3.77	4.88	0.77	-	[8]

E. Radiative properties

The Ω_λ values obtained from the absorption measurements have been used to calculate the radiative transition probability, branching ratios and radiative lifetime of the excited state $^4F_{3/2}$.

The radiative transition probability $A(aJ, bJ')$ for the emis-

sion from initial state aJ to a final state bJ' for an electric dipole emission has been determined using the relation [26]

$$A(aJ, bJ') = \frac{64\pi^4 e^2}{3h\lambda_o^3(2J+1)} \frac{n(n^2+2)^2}{9}$$

TABLE VIII: Radiative transition probability (A), total transition probability (A_T), radiative lifetime (τ_R) and branching ratio (β_R) for the excited $^4F_{3/2}$ of Nd^{3+} ion in sodium lead borate glasses.

Transitions from $^4F_{3/2} \rightarrow$	NPBN1		NPBN2		NPBN3		NPBN4		NPBN5		Borate Glass [30]	Lead Borate [8]
	$A(s^{-1})$	β_R	$A(s^{-1})$	β_R	$A(s^{-1})$	β_R	$A(s^{-1})$	β_R	$A(s^{-1})$	β_R	β_R	β_R
$^4I_{15/2}$	10	0.005	15	0.005	17	0.005	18	0.005	19	0.005	0.005	0.005
$^4I_{13/2}$	197	0.097	291	0.106	324	0.107	345	0.100	363	0.101	0.009	0.101
$^4I_{11/2}$	975	0.483	1388	0.506	1541	0.508	1691	0.490	1770	0.492	0.490	0.506
$^4I_{9/2}$	835	0.414	1047	0.382	1151	0.379	1398	0.405	1442	0.401	0.420	0.388
$A_T(s^{-1})$	2016		2742		3033		3452		3594		2386	3273
$\tau_R(\mu s)$	496		365		330		290		278		419	306
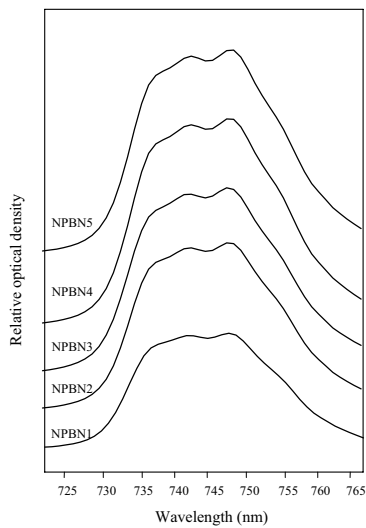
FIG. 4: Spectral profile of the transition $^4I_{9/2} \rightarrow {}^4F_{7/2}$, $^4S_{3/2}$ for various concentrations of Nd_2O_3 in sodium-lead-borate glasses.

$$\sum_{\lambda=2,4,6} \Omega_\lambda \left| \left\langle (S,L)J \left\| U^{(\lambda)} \right\| (S',L')J' \right\rangle \right|^2 \qquad (9)$$

where λ_o is the peak wavelength of the emission bands.

The total radiative emission probability $A_T(aJ)$ of an excited state is given by the sum of the $A(aJ,bJ')$ terms calculated over all the terminal states b.

$$A_T(aJ) = \sum_{bJ'} A(aJ,bJ') \qquad (10)$$

The fluorescence branching ratio β_R has been determined using:

$$\beta_R = \frac{A(aJ,bJ')}{A_T(aJ)} \qquad (11)$$

The radiative lifetime τ_R of the emission state is given as

$$\tau_R = \frac{1}{A_T(aJ)} \qquad (12)$$

Radiative transition probability (A), total transition probability (A_T), radiative lifetime (τ_R) and branching ratio (β_R) for the excited $^4F_{3/2}$ are summarized in Table 8. A comparison of (β_R) with vitreous borate [30] and lead borate [8] glasses has been made in the same table. The Ω_2 parameter becomes independent in characterizing the fluorescence properties of $^4F_{3/2} \rightarrow {}^4I_J$ transitions because the values of tensor operator $\left\| U^2 \right\|^2$ are zero for all these transitions. Hence, the radiative properties depend on Ω_4 and Ω_6 parameters because of the triangle rule $|J-J'| \leq \lambda \leq |J+J'|$ [27]. The $^4F_{3/2} \rightarrow {}^4I_{11/2}$ transition is the potential lasing transition (λ=1.06μm) for Nd^{3+} ion. The radiative transition probability is found to increase with increase in content of Nd_2O_3. It shows a maximum for NPBN5 i.e. the glass containing 2 mol% concentration of Nd_2O_3. The radiative lifetime is inversely proportional to the linear combination of Ω_4 and Ω_6 [28]. Thus, the lowering trend noticed in τ_R on increasing rare earth concentration has been attributed to the increasing values of Ω_4 and Ω_6 parameters.

IV.   CONCLUSIONS

We have determined physical and spectroscopic properties for sodium-lead-borate glasses doped with varying amounts of Nd^{3+}. Density measurements predict the formation of non-bridging oxygen atoms around 1.75 mol% concentration of Nd_2O_3. The indirect and direct mobility gap both show a maximum for 2 mol% and a minimum for 1mol% concentration of Nd_2O_3. Absorption spectra have been analyzed using the Judd-Ofelt theory. The Ω_2 parameter and hence the non-symmetric component of electric field acting on Nd^{3+} ion is found to be highest for 1.75 mol% of Nd_2O_3. The position and shape of the hypersensitive transition does not change ap-preciably. Therefore, the covalency of the Nd-O bond has been determined from the spectral profile of the $^4I_{9/2} \rightarrow ^4F_{7/2}$, $^4S_{3/2}$ transition. A higher value of intensity ratio I_L/I_S and intensity parameter Ω_6 indicates highest covalency of the Nd-O bond for glass containing 2 mol% of Nd_2O_3. The spectroscopic quality factor $X = \Omega_4/\Omega_6$ is found to be 2–3 times larger than that of the standard laser host for Nd^{3+}, namely YAG with X=0.3. A maximum of radiative transition probability and a minimum of radiative lifetime are observed for glass containing 2 mol% of Nd_2O_3. The variation of the spectroscopic properties suggests that it is possible to enhance the lasing properties of Nd^{3+} in sodium-lead-borate glasses by varying the concentration of the rare-earth ions.

[1] Y. Nageno, H. Takebe, and K. Morinaga, J. Am. Ceram. Soc. **76**, 3081 (1993).

[2] A. R. Devi, C. K. Jayasankar, Mater. Chem. Phys. **42**, 106 (1995).

[3] V. Mehta, G. Aka, A. L. Dawar, and A. Mansingh, Opt. Mater. **12**, 53 (1999).

[4] E. Pecoraco, J. A. Sampaio, L. A. O. Nunes, S. Gama, and M. L. Baesso, J. Non-Cryst. Solids. **277**, 7 (2000).

[5] N. Soga, K. Hirao, M. Yoshimoto, and H. Yamamoto, J. Appl. Phys. **63**, 4451 (1988).

[6] S. M. Kaczmarek, Opt. Mat. **19**, 189 (2002).

[7] J. Zhong and P. J. Bray, Change in boron coordination in alkali borate glasses and mixed alkali effects, as elucidated by NMR, J. Non-Cryst. Solids **111**, 67 (1989).

[8] M. B. Saisudha, J. Ramakrishna, Phys. Rev. B **53**, 6186 (1996).

[9] M. B. Saisudha, K. S. R. K. Rao, H. L. Bhat, and J. Ramakrishna, J. Appl. Phys. **80**, 4845 (1996).

[10] S. Mukhopadhyay, K. P. Ramesh, R. Kannan, and J. Ramakrishna, Phys. Rev. B **70**, 224202 (2004).

[11] Y. C. Ratnakaram, R. P. S. Chakradhar, K. P. Ramesh, J. L. Rao, and J. Ramakrishna, J. Phys. Cond. Matt. **15**, 6715 (2003).

[12] A. S. Rao, Y. N. Ahammed, R. R. Reddy, and T. V. R. Rao, Opt. Mater. **10**, 245 (1998).

[13] A. S. Budi, R. Hussin, and M. R. Sahar, Electrical properties of neodymium phosphate glass semiconductor electronics, Proceedings ICSE, **19**, 247 (2002).

[14] N. F. Mott, E. A. Davis, *Electronic processes in non-crystalline materials*, Clarendon Press (1979).

[15] F. Urbach, Phys. Rev. **92**, 1324 (1953).

[16] J. Tauc, J. Non-Cryst. Solids **149**, 97 (1987).

[17] G. H. Dieke, *Spectra and Energy Levels of Rare Earth Ions in Crystals*, Interscience, New York (1968).

[18] E. Y. Wong, J. Chem. Phys. **35**, 544 (1961).

[19] Y. C. Ratnakaram, A. Vishwanadha Reddy, J. Non-Cryst. Solids **277**, 142 (2000).

[20] B. R. Judd, Phys. Rev. **127**, 750 (1962).

[21] G. S. Ofelt, J. Chem. Phys. **37**, 511 (1962).

[22] W. T. Carnall, P. R. Fields, and K. Rajnak, J. Chem. Phys. **49**, 4424 (1968).

[23] C. K. Jorgensen, B. R. Judd, Mol. Phys. **8**, 281 (1964).

[24] R. D. Peacock, *Structure and Bonding*, vol. 22, Springer, Berlin, (1975).

[25] W. F. Krupke, Phys. Rev. **145**, 325 (1966).

[26] D. C. Brown, *High Peak Power Nd: Glass Laser Systems*, Springer, Berlin, (1981).

[27] Y. C. Ratnakaram, N. Sudharani, J. Phys. Chem. Solids **59**, 215 (1998).

[28] M. J. Weber, J. D. Meyers, and D. H. Blackburn, J. Appl. Phys. **52**, 2944 (1981).

[29] H. Takebe, K. Morinaga, and T. Izumitani, J. Non-Cryst. Solids, **178**, 58 (1994).

[30] R. Reisfeld, C. K. Jorgensen, *Lasers and excited states of rare earths*, Springer, New York, (1977).